Modelling of long-term hygro-thermal behaviour of vacuum insulation panels

A. Batard, T. Duforestel, Flandin Lionel, B. Yrieix

Energy & Buildings 173 (2018) 252–267

Contents lists available at ScienceDirect

Energy & Buildings

journal homepage: www.elsevier.com/locate/enbuild

Modelling of long-term hygro-thermal behaviour of vacuum insulation panels

A. Batard[a,b,1,*], T. Duforestel[a,2], L. Flandin[b,3], B. Yrieix[c]

[a] EDF Lab Les Renardières, 77250 Morêt Loing et Orvanne, France
[b] LEPMI – LMOPS, Université de Savoie – Campus Savoie Technolac, Hélios – 73376 Le Bourget-du-Lac, France
[c] EDF Lab Les Renardières, 77250 Morêt Loing et Orvanne, France

ARTICLE INFO

Article history:
Received 23 November 2017
Revised 12 March 2018
Accepted 19 April 2018
Available online 18 May 2018

Keywords:
Vacuum insulation panels
Core material behaviour
Gas permeation
Heat transport
Modelling

ABSTRACT

The low thermal conductivity of Vacuum Insulation Panels (VIPs) degrades with time due to gas permeation through VIPs barriers. There is additional ageing of their envelope and core material. Accelerated experiments are carried out in order to better understand this ageing process but they are not sufficient to predict the long term performance of panels. Models have to be used to connect the short term evaluation and the long term behaviours in order to improve the prediction of the thermal conductivity evolution over 50 years. This paper describes the development of a VIP model in the Dymola® software. This model takes into account the envelope and core material hydro-thermal characteristics and behaviours, and integrates the actual solicitations of the panels during accelerated ageing tests. The thermo-activation of the envelope permeance is integrated. Many properties of the core material are modelized: type of core material, sorption isotherm, hygro-thermal ageing, pore size distribution, etc. Simulations in constant conditions in temperature and humidity have been carried out. The results show that the real behaviour of the VIPs conductivity can't be simply evaluated through a linear extension of its short-term evolution. Given the important impact of the core material detailed characteristics, it is absolutely necessary to get an accurate determination of the core material sorption curve and of the ageing of this curve.

1. Introduction

Vacuum Insulation Panels (VIP) is a super-insulated product consisting of a core material maintained under vacuum by an envelope. Its thermal performance is based on the nanoporous property of the core material and on the barrier envelope efficiency which prevents the increase of moisture and internal pressure (cf. Fig. 1).

Different types of VIPs exist with different core materials and envelopes. At initial state, the mean thermal conductivity of VIPs made with nanoporous silica is around 4 mW m^{-1} K^{-1} at the center of panel. In practice, its thermal performance is not stable but increases with time due to gas permeation through VIPs barriers and ageing of their envelope [1,2] and core material [3–6]. The global thermal conductivity of the panel depends on many physical characteristics of the core materials, and on their interactions with gases (dry air and water vapour) [7–10]. To commercialize VIPs for building insulation application, it is necessary to estimate their long-term mean thermal performance. Several authors have proposed methods to model the changes in thermal conductivity of panels [11–17]. These predictions are commonly realised by making simplifications and for most of them, without taking into account, that also barrier complex as well as core do change over time.

The aim of this study is to develop a VIP model and simulate, over a 50-year period and as accurately as possible, its hygro-thermal behaviour. This in order to analyse its thermal performance when subjected to different temperature and humidity conditions. The paper is split in seven parts. First, methods and modelling tools are presented. Then, the different equations on which the model is based are described. The two next parts are devoted to the sensibility analysis and the presentation of the simulation results in constant climatic conditions. The fifth part describes how

* Corresponding author.
E-mail addresses: antoine.batard@edf.fr (A. Batard), thierry.duforestel@edf.fr (T. Duforestel), lionel.flandin@univ-savoie.fr (L. Flandin), bernard.yrieix@edf.fr (B. Yrieix).
[1] PhD.
[2] Company Tutor.
[3] Advisor Thesis.

https://doi.org/10.1016/j.enbuild.2018.04.041

Nomenclature

Greek letters

α	Parameter of the rate of ageing –
β	Non-dimensional coefficient –
λ_c	Core material's thermal conductivity W m^{-1} K^{-1}
λ_f	Barrier complex's thermal conductivity, in transversal direction W m^{-1} K^{-1}
λ_g	Gaseous thermal conductivity W m^{-1} K^{-1}
λ_r	Radiative thermal conductivity W m^{-1} K^{-1}
λ_s	Solid thermal conductivity W m^{-1} K^{-1}
λ_{cs^0}	Initial solid thermal conductivity W m^{-1} K^{-1}
λ_{eq}	Equivalent VIP's thermal conductivity W m^{-1} K^{-1}
$\lambda_{f,\,i}$	Thermal conductivity of the barrier complex layer *i*, in transversal direction W m^{-1} K^{-1}
λ_{g^0}	Gaseous thermal conductivity of not confined gas W m^{-1} K^{-1}
λ_{memb}	Apparent thermal bridge conductivity W m^{-1} K^{-1}
λ_{sil}	Solid thermal conductivity of non-porous silica W m^{-1} K^{-1}
λ_{VIP}	Global VIP's thermal conductivity W m^{-1} K^{-1}
ϕ	Relative humidity %
Φ_i	Mass flow of gas *i* kg s^{-1}
Φ_{memb}	Heat flow of the linear thermal bridge *W*
Π_i	Apparent permeance to the gas *i* kg m^{-2} s^{-1} Pa^{-1}
Ψ_{memb}	Linear thermal bridge coefficient W m^{-1} K^{-1}
ρ	Density or mass concentration kg m^{-3}
τ_w	Mass content of water %
ε	Porosity –
φ_i	Mass flow density of gas *i* kg s^{-1}

Other symbols

Ø	Pore mean size m

Physical constants

σ	Stefan-Boltzmann's constant 5.67 × 10^{-8} W m^{-2} K^{-4}
C	Constant depending on gas J K^{-1} m^{-2}
k_B	Boltzmann's constant 1.381 × 10^{-23} J K^{-1}
R	Ideal gas constant 8.314459848 J K^{-1} mol^{-1}
r_i	Specific gas constant of gas i J kg^{-1} K^{-1}

Roman letters

A	Panel's area m^2
B	Influence of water content increase on the thermal conductivity W m^{-1} K^{-1}%$^{-1}$
d	Panel's thickness m
d_c	Core material's thickness m
d_g	Effective diameter of gas molecule m
D_i	Diffusion coefficient of gas *i* m^2 s^{-1}
E	Extinction coefficient m^{-1}
G	Influence of pressure increase on the thermal conductivity W m^{-1} K^{-1} Pa^{-1}
h_i	Convection heat transfer coefficients W m^{-2} K^{-1}
I_i	Sensitivity index of input i %
k_i	Fitting parameters for sorption isotherm model –
l	Barrier complex's thickness m
l_i	Thickness of the barrier complex layer *i* m
m_{ads}	Mass of adsorbed water kg
M_{H_2O}	Molar mass of water kg mol^{-1}
m_{sil}	Mass of dry core material kg
m_w	Mass of water kg
m_{wv}	Mass of water vapour kg
n	Refractive index –
n_l	Number of layers of the edge –
P	Panel's perimeter m
p_a	Partial pressure of dry air Pa
p_t	Internal total pressure Pa
p_v	Partial pressure of water vapour Pa
Q_D	Activation energy of diffusion J mol^{-1}
Q_S	Activation energy of sorption J mol^{-1}
Q_Π	Activation energy of permeance J mol^{-1}
R_c	Core material's thermal resistance K m W^{-1}
R_f	Barrier complex's thermal resistance K m W^{-1}
R_{eq}	Equivalent VIP's thermal resistance K m W^{-1}
R_{memb}	Apparent thermal bridge resistance K m W^{-1}
S	Solubility coefficient kg m^{-3} Pa^{-1}
S_{BET}	BET Specific surface area m^2 kg^{-1}
T	Temperature K
t	Time s
t_{aged}	Time for which the silica is fully aged s
V	Variance contribution –
V_{VIP}	VIP's volume m^3
Var	Variance –
X_i	Model input variable –
Y_i	Model output variable –

the silica ageing has been implemented in the modelling process and its impact on the long-term thermal behaviour of the panels. The sixth part is devoted to the model validation and discussion about traditional ageing prediction. Then, the last part is devoted to the conclusion.

2. Methods and modelling tools

Dymola® platform has been used to develop the model in the Modelica modelling language. This software has been developed to simulate the dynamic behaviour and complex interactions between systems in various engineering fields.

The developed model consists of an assembly of six macro-components: two barrier complexes, one core material, one thermal bridge and two convective heat exchangers. All components are interconnected with ports. The whole system is further submitted to boundary conditions that mimic external exchange. Each port carries three potential variables: temperature, water vapour partial pressure and total gas pressure; and three flux associated to these three potentials: heat flow, water vapour mass flow and total mass flow. Each component behaviour is described by physical equations and necessary parameters.

A schematic illustration of the model is represented in Fig. 2. The model takes into account the thermal behaviour and gas transfer through the complex and in the core material.

3. Physical model description

3.1. Thermal transfer modelling

3.1.1. Panel

The overall thermal behaviour of the VIP can be represented with a set of series-parallel thermal resistances (cf. Fig. 3).

In practice, the thermal resistance of the complex barriers (R_f) can be neglected. The equivalent thermal resistance of the panel can result in two parallel resistances (Eq. (1)) : the resistance of the core material (R_c), and that of the thermal bridge of the envelope (R_{memb}).

$$\frac{1}{R_{eq}} = \frac{1}{R_c} + \frac{1}{R_{memb}} \tag{1}$$

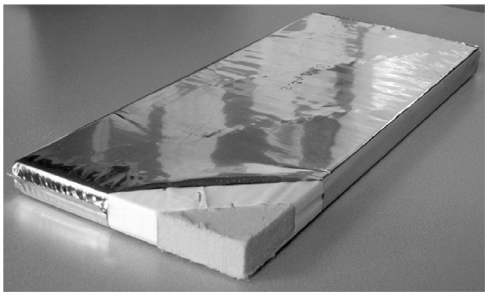

Fig. 1. Vacuum Insulation Panel (VIP).

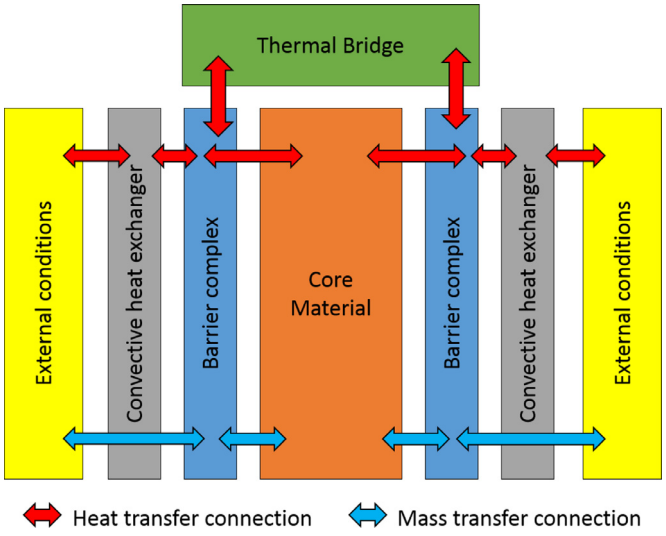

Fig. 2. Schematic illustration of the VIP model.

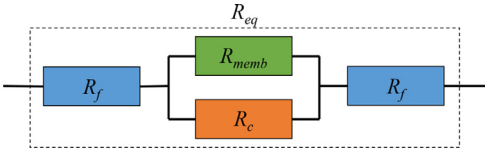

Fig. 3. Equivalent thermal resistance of the panel.

It is common to consider the resistance as equal to the thickness divided by the thermal conductivity (Eq. (2)).

$$\frac{1}{R_{eq}} = \frac{d}{\lambda_{eq}} \tag{2}$$

It is possible to deduce that:

$$\frac{\lambda_{eq}}{d} = \frac{1}{R_c} + \frac{1}{R_{memb}} \tag{3}$$

$$\lambda_{eq} = \frac{d}{R_c} + \frac{d}{R_{memb}} \tag{4}$$

Because panels thickness can be assimilated to core materials thickness ($d_c \approx d$), the core material thermal conductivity is equal to:

$$\lambda_c = \frac{d_c}{R_c} \approx \frac{d}{R_c} \tag{5}$$

By assuming that:

$$\lambda_{memb} = \frac{d}{R_{memb}} \tag{6}$$

Panel thermal conductivity can be written as a function of the core material thermal conductivity and the thermal bridge of the complex barrier (Eq. (7)).

$$\lambda_{eq} = \lambda_c + \lambda_{memb} = \lambda_{VIP} \tag{7}$$

As every linear thermal bridge, the heat flow due to the membrane can be calculated with a linear thermal bridge coefficient (Eq. (8)).

$$\Phi_{memb} = \Psi_{memb} P \Delta T \tag{8}$$

According to the relation between the heat flow and the thermal conductivity (Eq. (9)), the thermal bridge can be written as below (Eq. (10)).

$$\Phi_{memb} = \frac{\lambda_{memb}}{d} A \Delta T \tag{9}$$

$$\lambda_{memb} = \frac{Pd}{A} \Psi_{memb} \tag{10}$$

Linear thermal bridge coefficient is calculated by the analytical model developed by Tenpierik and Cauberg [15] which takes into account the thermal drainage effect (Eq. (11)).

$$\Psi_{memb} = \frac{1}{\frac{d}{n_l l \lambda_f} + \frac{1}{\sqrt{h_1 l \lambda_f}} + \frac{1}{\sqrt{h_2 l \lambda_f}}} \tag{11}$$

As mentioned above, in practice the equivalent thermal conductivity of the barrier complex, in transversal direction, can be neglected. But to calculate the linear thermal bridge coefficient, thermal conductivity of the envelope can be calculated using the combining rules of layers in series (Eq. (12)).

$$\lambda_f = \frac{l}{\sum_i \frac{l_i}{\lambda_{f,i}}} \tag{12}$$

3.1.2. Core material

Core material is discretised in several layers in order to take into account the temperature gradient through the thickness. Heat transfer in a porous media is commonly represented by the parallel flux model [7–9,18–22]. The total core material thermal conductivity can be split into three contributions: radiative, solid and gaseous conduction.

$$\lambda_c = \lambda_r + \lambda_s + \lambda_g \tag{13}$$

Initial radiative and solid contributions can be measured and considered as model inputs [21]. But without measurement, radiative conduction is calculated through the Rosseland approximation (Eq. (14)). It is supposed to depend only on the temperature:

$$\lambda_r(T) = \frac{16}{3} \frac{\sigma n^2 T^3}{E(T)} \tag{14}$$

Solid conduction is calculated from the dry thermal conductivity and the mass of water adsorbed (Eq. (15)):

$$\lambda_s(T, \phi) = \lambda_{cs}^0(T) + B\tau_w(\phi) \tag{15}$$

The B coefficient is an experimental parameter that represents the thermal conductivity increase due to water adsorption of the core material. Dry thermal conductivity depends on material structure and porosity. In the case of a porous silica, the Kamiuto's model [23] is used to calculate the solid thermal conductivity of non-porous silica and then the porous one (Eqs. (16) and (17)). These equations have been deduced from measurements. The radiative contribution have been deducted from the total thermal conductivity measured under vacuum.

$$\lambda_{sil}(T) = -4,22.10^{-6} T^2 + 4,3633.10^{-3} T + 0,442 \tag{16}$$

$$\lambda_{cs}^0(T) = (1 - \varepsilon) e^{-(9,298 - 6,91\varepsilon)\varepsilon} \lambda_{sil}(T) \tag{17}$$

The relation between the water content and the relative humidity in the pores is given by the core material sorption isotherms:

$$\tau_w = f(\phi) \tag{18}$$

In practice, for mineral core material, sorption isotherms are supposed independent from the temperature. Several models of sorption isotherms can be found in the literature. The GAB's model, thoroughly described in [24], is the most appropriate. For silica core materials, the model suggested in IEA Annex 39 [25] has been chosen and its implementation is described in Sections 5 and 6. The gaseous conduction is represented using Knudsen's relation developed by Kaganer [26]. It depends on temperature, porosity, pressure and pore mean size. It is possible to integrate a pore size distribution and not only one mean value:

$$\lambda_g(T, p_t) = \varepsilon \frac{\lambda_g^0(T)}{1 + \frac{CT}{\varnothing p_t}} \tag{19}$$

$$C = \sqrt{2}\beta \frac{k_B}{\pi d_g^2} \tag{20}$$

Then, the global thermal conductivity of the panel can be written with the following general formula:

$$\begin{aligned} \lambda_{VIP}(T, \phi, p_t) \quad = \quad & \frac{16}{3}\frac{\sigma n^2 T^3}{E(T)} + \lambda_{cs}^0(T) + B\tau_w(\phi) \\ & + \varepsilon \frac{\lambda_g^0(T)}{1 + \frac{CT}{\varnothing p_t}} + \frac{Pd}{A}\Psi_{memb} \end{aligned} \tag{21}$$

3.2. Mass transfer modelling

3.2.1. Diffusion through the barrier

The role of the VIP barrier is to maintain the core material under vacuum thanks to his low permeance to humidity and atmospheric gases. Metalized multilayer films or laminated films can be considered in this model. The membrane is considered as an equivalent homogeneous material. The model used for each gas diffusion though the membrane is the sorption-diffusion model. It is commonly considered for polymers by many authors [27–29]. Dissolution takes place on each side of the membrane using Henry's law. And diffusion though the material is governed by Fick's laws. The total flow Φ_i of a gas i is composed of a surface term (gas flow through the current portion of the barrier) and a linear term (gas flow through the perimetric welding of the barrier) (Eq. (22)). Surface and linear flow are calculated thanks to macroscopic quantities which are the apparent surface and linear permeances (Eq. (23)). The total gas flow depends on the membrane surface and perimeter, the permeances and the pressure difference between the two faces.

$$\Phi_i = A\Phi_{i,surf} + P\Phi_{i,lin} \tag{22}$$

$$\Phi_i = (A\Pi_{i,surf} + P\Pi_{i,lin})\Delta p_i \tag{23}$$

The permeance is defined as the product of the diffusion and solubility coefficients divided by the barrier complex thickness (Eq. (24)).

$$\Pi = \frac{DS}{l} \tag{24}$$

Thermo-activation of these two coefficients can be represented by the Arrhenius's law (Eqs. (25) and (26)).

$$D = D_0 e^{\frac{Q_D}{RT}} \tag{25}$$

$$S = S_0 e^{\frac{Q_S}{RT}} \tag{26}$$

By mixing Eqs. (24)–(26), each apparent permeance can be written as shown in Eq. (27).

$$\Pi = \frac{D_0 e^{\frac{Q_D}{RT}} S_0 e^{\frac{Q_S}{RT}}}{l} \tag{27}$$

It is possible to obtain the relations below:

$$\Pi_0 = \frac{D_0 S_0}{l} \tag{28}$$

$$e^{\frac{Q_\Pi}{RT}} = e^{\frac{Q_D}{RT}} e^{\frac{Q_S}{RT}} \tag{29}$$

Diffusion and solubility reference coefficients and their activation energies (Eq. (27)) can directly be a model inputs, or apparent permeances can be calculated from apparent reference permeances and activation energies (Eq. (30)).

$$\Pi = \Pi_0 e^{\frac{Q_\Pi}{RT}} \tag{30}$$

3.2.2. Core material

Given the very slow pace governing the gas transfer through the barrier, the gas equilibrium in the core material can be considered as very fast. But, it is necessary to integrate water vapour diffusion because there are variations of water vapour saturation pressure and a gradient of water content because of temperature gradient. Gas diffusion is taken into account through the different layers of the core material thanks to the Fick's law.

$$\overrightarrow{\varphi_v} = -D_v \overrightarrow{\nabla} \rho_v \tag{31}$$

In the ports of our models, the mass potential is not density but partial pressure. So, the equation is rewritten according to the pressure and respecting the ideal gas law (Eqs. (32) and (33)):

$$p_v = \rho_v r_v T \Leftrightarrow \rho_v = \frac{p_v}{r_v T} \tag{32}$$

$$\overrightarrow{\varphi_v} = -\frac{D_v}{r_v T} \overrightarrow{\nabla} p_v \tag{33}$$

The same equations are implemented in the models for dry air diffusion (Eq. (34)), but it can be considered as instantaneous.

$$\overrightarrow{\varphi_a} = -\frac{D_a}{r_a T} \overrightarrow{\nabla} p_a \tag{34}$$

4. Sensibility analysis

A sensitivity analysis is carried out in order to globally evaluate the relationships between input and output variables of the model. Through this study it is possible to identify input variables for which measurement accuracy is most important.

Five input variables are studied. First, water vapour and dry air permeances of the barrier complex are selected because the panel performance is based on the capacity of barrier complex to maintain vacuum. The low thermal conductivity of panel is also due to the Knudsen effect and this is why porosity and mean pore size of the core material are chosen. And then, it is important to study the B coefficient because this input determine the impact of water content on the thermal conductivity. The other input variables are not studied because they don't have a direct link on the hygrothermal behaviour of the panel when it is ageing. Each input can take three or four values included between the lower-range and the upper-range values that have been found in the published scientific literature. The Table 1 summarizes all the studied input values.

The reference barrier complex is a V08621B film from Hanita®. Its water vapour and dry air permeance reference values measured on panels are fixed for 23 °C to 1.31×10^{-14} and 1.29×10^{-18} kg m^2 s^{-1} Pa^{-1} respectively [30]. These values are global

Table 1
Input variables values.

Inputs	ϵ	$\varnothing$	B	Π_{wv} Π_{air}
Units	%	nm	mW m^{-1} K^{-1}%$^{-1}$	kg m^{-2} s^{-1} Pa^{-1}
Value 1	90	50	0.14	0.1 × Π_{ref}
Value 2	95	200	0.3	0.5 × Π_{ref}
Value 3	98	350	0.5	1 × Π_{ref}
Value 4	–	–	1	2 × Π_{ref}

permeances including surface term (gas flow through the current portion of the barrier) and a linear term (gas flow through the perimetric welding of the barrier). The surface and linear permeances don't have the same units, but according to literature [30–32], water vapour linear permeance can be set at one third of the surface permeance. Dry air linear permeance is set at the triple of the surface permeance. Activation energies for surface and linear permeances are fixed to 26 kJ mol^{-1} for water vapour [33], and 30 kJ mol^{-1} for dry air [29,32,34]. Core material characteristics are those with core material C2 which is more detailed on Section 5.

The studied output variables are: initial thermal conductivity and mean thermal conductivities at different stages of the ageing process (after 10, 20, 30, 40 and 50 years). The impact of each input on each mean thermal conductivity is analysed. 576 simulations are realised over 50 years in three temperature and relative humidity conditions: 20 °C/40%, 40 °C/70% and 70 °C/90%.

The sensitivity indices I_{X_i} for each input variables X_i and I_{X_i} : X_j for each interaction effects X_i: X_j, are calculated from analysis of variance (ANOVA). This method consider that the total variance $Var[Y(X)]$ of an output Y can be decomposed into factors directly caused by inputs V_{X_i}, and others V_{X_i} : X_i caused by their interaction (Eq. (35)). The sensitivity indices are calculated by dividing each variance contribution by the total variance (Eq. (36)).

$$Var[Y(X)] = \sum_i V_{X_i} + \sum_{i,j} V_{X_i:X_j} \tag{35}$$

$$I_{X_i} = \frac{V_{X_i}}{Var[Y(X)]} \text{ and } I_{X_i:X_j} = \frac{V_{X_i:X_j}}{Var[Y(X)]} \tag{36}$$

Fig. 4 shows indices calculated with R software and regarding the six output variables, for each testing condition. Only indices higher than 1% are represented.

The initial thermal conductivity only depends on porosity, with an index larger than 99%. In contrast during the ageing, the sensitivity indices due to porosity decrease, while Π_{air} (for rather dry conditions), B and Ø(for wetter conditions) become influential. In addition, the interactions between input variables have no significant impact on the outputs and can be neglected.

In rather dry conditions (20 °C/40% RH), porosity always controls at least half of the variability. Nevertheless the mean thermal conductivity becomes gradually altered by dry air permeance, mean pore size and water vapour permeance. Over 50 years, the mean thermal conductivities are respectively responsible for 28%, 11% and 8% of the model variability. In these rather dry conditions, the variability due to the B coefficient is insignificant.

At 40 °C/70% RH, porosity explains less than 56% of the variability over 10 years. This index decreases to 19% for the mean thermal conductivity calculated over 50 years. In short term, the mean thermal conductivity depends more on water vapour permeance than in long term. The inverse evolution can be observed for dry air permeance, mean pore size and B coefficient. Over 50 years, the mean thermal conductivity is more sensitive to dry air permeance (31%), mean pore size (23%) and B coefficient (11%) than to water vapour permeance (10%).

In wet conditions (70 °C/90% RH), the impact of porosity is always less than 12%. The mean pore size and the B coefficient are

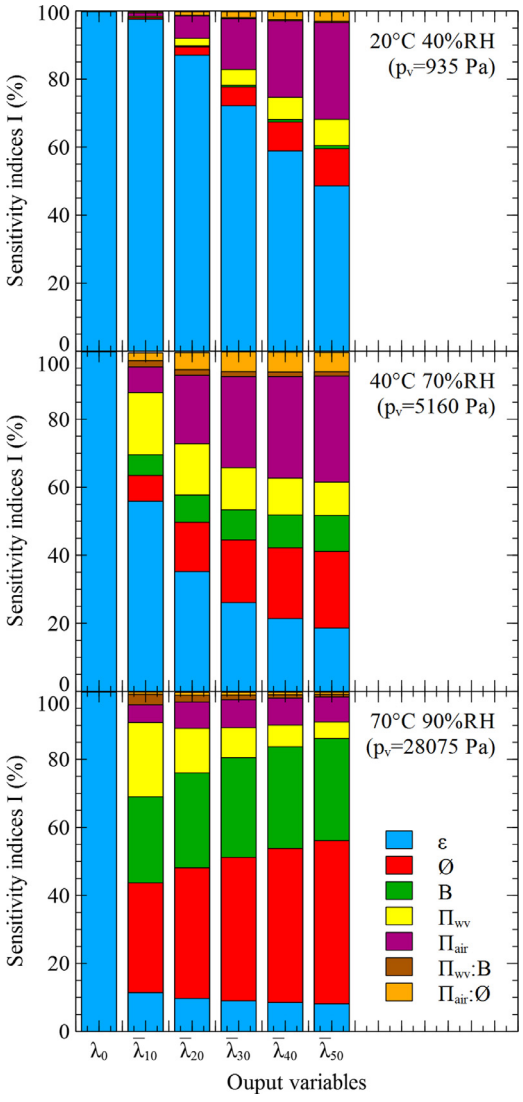

Fig. 4. Sensitivity index of the model regarding mean thermal conductivity at different age and in three hygro thermal conditions: 20 °C/40%, 40 °C/70% and 70 °C/90%.

inputs which have the greatest impact on the mean thermal conductivity variability. Their effects increase when the mean thermal conductivity is calculated over a longer time period. The impact of mean pore size represents between 32 and 49% of the variability, while the impact of the B coefficient is between 25 and 30%. The permeance effects are surprisingly low and clearly exceeded by the previous parameters. Nevertheless, it can be observed that in time, the impact of water vapour permeance tends to decrease (from 22 to 4%), while the impact of the dry air permeance tends to increase (from 4 to 8%).

5. Simulation results in constant conditions with different porous silica core materials

Simulations in constant conditions are carried out in order to study the influence of several temperature and humidity solicitations on thermal conductivity of VIP' panels with different core materials. Three VIPs with the same envelope but different core material are studied: C1, C2 and C3. The barrier complex is typically a tri-metallize V08621B film from Hanita®. Its water vapour and dry air permeance values and the activation energies are the same than those used in Section 4 for the sensitivity analysis. Two

Table 2
Silica characteristics.

Silica	Type	S_{BET} (m^2 g^{-1})	ρ (kg m^{-3})
S1	Hydrophobic fumed	170 ± 20	365
S2	Hydrophilic fumed	200 ± 25	185
S3	Hydrophilic precipitated	250 ± 30	265

Table 3
Fitting parameters for the water vapour sorption isotherms of studied silica (at initial state).

Silica	k_1	k_2	k_3	k_4
S1	0.00777	1.83109	0.70576	5.43698
S2	0.11178	5.67065	2.90451	4.94117
S3	0.08714	0.06000	2.26808	4.99399

Table 4
Water vapour partial pressure for each condition.

Conditions	40 % RH	70 % RH	90 % RH
20 °C	935 Pa	1636 Pa	2103 Pa
40 °C	2948 Pa	5160 Pa	6634 Pa
70 °C	12,478 Pa	21,836 Pa	28,075 Pa

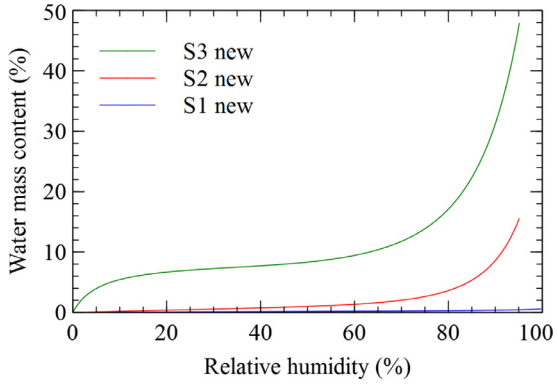

Fig. 5. Water vapour sorption isotherms at 25 °C of new silica S1, S2 and S3.

fumed and one precipitated silica are used. They are named silica S1, S2 and S3 in this study. Their main characteristics, according to the suppliers' information, are given in Table 2.

Silica S1 is a hydrophobic fumed silica obtained from the treatment of the hydrophilic fumed silica S2. silica S3 is a precipitated silica and is much more hydrophilic. Porosity is fixed to 80%, 88% and 92% for silica S1, S2 and S3 respectively and their mean pore size around 260 nm.

Water vapour sorption isotherms have been measured for all silica at initial state. The fitting curve suggested in the Annex 39 [25] has been used (Eq. (37)).

$$\tau_w(\phi) = \frac{k_1 \cdot \phi}{k_2 + \phi} e^{k_3 \cdot \phi^{k_4}} \tag{37}$$

For the three testing core material, the fitting parameters are given in Table 3.

The obtained sorption isotherms at 25 °C are presented on Fig. 5.

The panels have been simulated for three temperatures (20 °C, 40 °C and 70 °C) and three relative humidities (40%, 70% and 90%) which resulted in nine different climatic conditions (cf. Table 4).

The initial conditions have been set to a temperature of 20 °C, a water vapour pressure of zero and total gas pressure of 100 Pa. The evolutions of the thermal conductivity avec 50 years are shown on Figs. 6–8 for each condition.

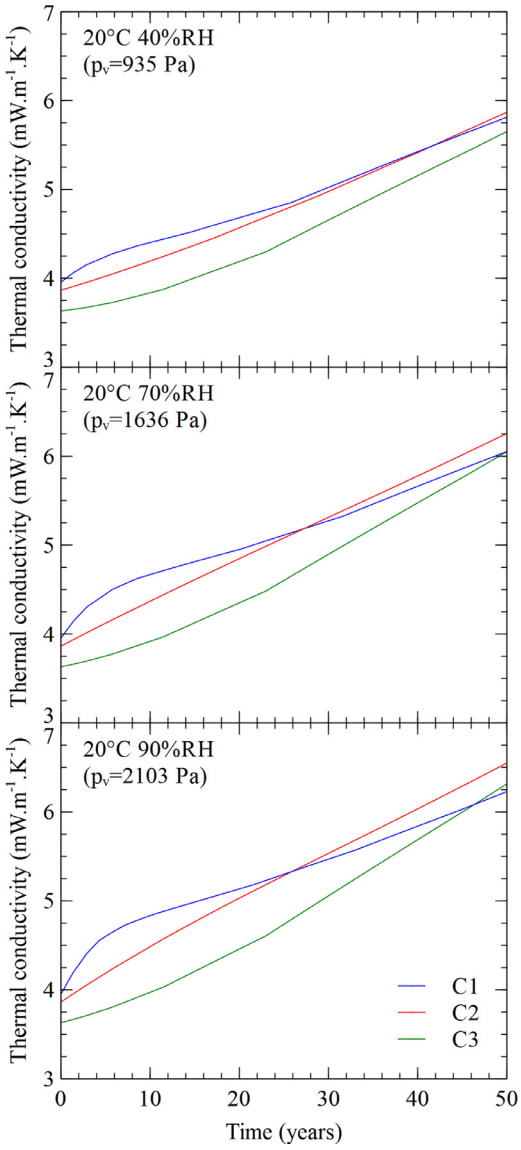

Fig. 6. Thermal conductivities evolution of VIPs aged over 50 years, at 20 °C and 40, 70 and 90% RH, with core materials C1, C2 and C3.

At 20 °C (cf. Fig. 6), all VIPs show a similar behaviour with a moderated thermal conductivity variation (≈2 mW m^{-1} K^{-1} over 50 years) whatever the relative humidity. The three core materials present different densities and therefore different initial thermal conductivities. Because larger densities reduce the radiative transfer while favouring solid conduction, an optimal value should balance these two phenomena. The density of core material C3 is actually closer to the optimum than the others core materials.

Thermal conductivity evolution seems to be linear for panel with core material C2 whatever the humidity. During the first years, an important increase of thermal conductivity can be observed for panel with core material C1 while this increase is much slower for core material C3. Thermal conductivity of panel with core material C3 always remains lower than the others during almost all the ageing. Nevertheless for the wetter configurations at 20 °C and 90% RH, the C3 conductivity curve can cross the C1 (after 45 years of ageing). The C1 conductivity curve also can cross the C2 curve.

As regards the hygric behaviour, C1 is the more hydrophobic core material and is rapidly saturated with water (cf. Fig. 9), while

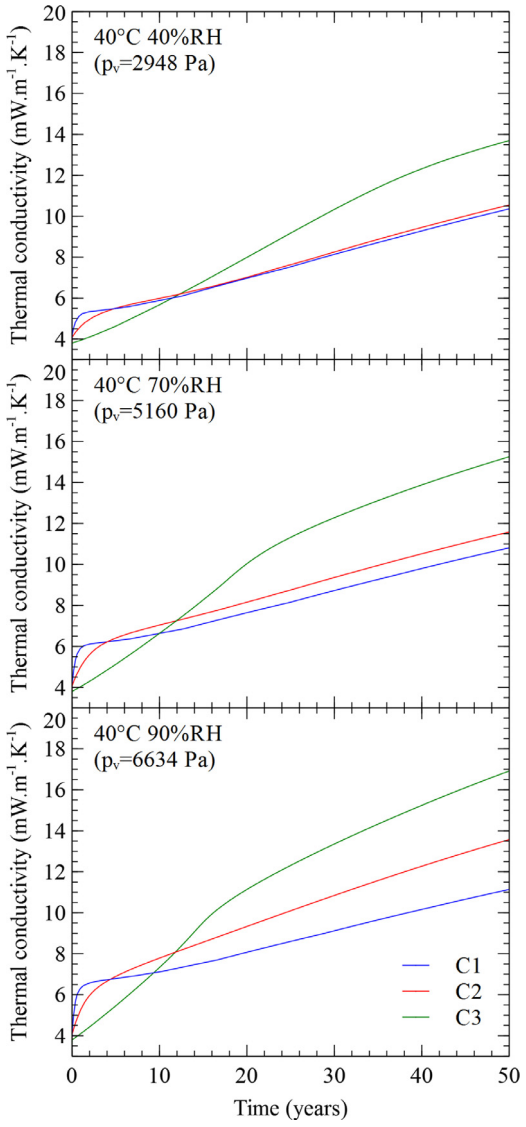

Fig. 7. Thermal conductivities evolution of VIPs aged over 50 years at 40 °C for 40, 70 and 90% RH, with core materials C1, C2 and C3.

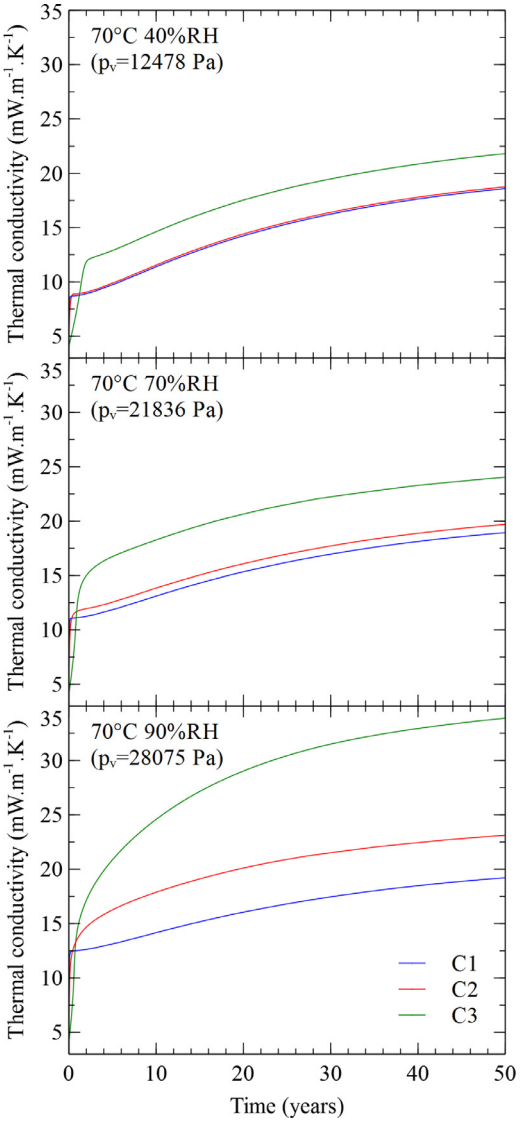

Fig. 8. Thermal conductivities evolution of VIPs aged over 50 years at 70 °C for 40, 70 and 90% RH, with core materials C1, C2 and C3.

C2 and C3 core matarials which are more hydrophilic, continue to adsorb moisture during the period.

Consequently, water vapour partial pressure in panel with core material C1 grows very rapidly until an equilibrium with the external water vapour partial pressure is reached (cf. Fig. 10).

Figs. 11 and 12 show the thermal conductivity contributions for core materials C1 and C3.

For core material C1 (cf. Fig. 11), gaseous conduction increases rapidly because of the important water vapour pressure increase, while the contribution due to adsorbed water remains very low. For a very hydrophobic core material, the influence of adsorbed water vapour on thermal conductivity can be neglected compared to the gaseous conduction. For a very hydrophilic core material (cf. Fig. 12 for C3), water adsorption maintains a low gas pressure and consequently a low gaseous conduction. More water vapour is adsorbed into core material but this alters less the thermal conductivity than gaseous water. Core material C2 behaviour is in between the two others. At 20 °C for all humidity conditions the water vapour partial pressure remains low (< 2100 Pa). Panels with the more hydrophilic core material can adsorb most of the incom-

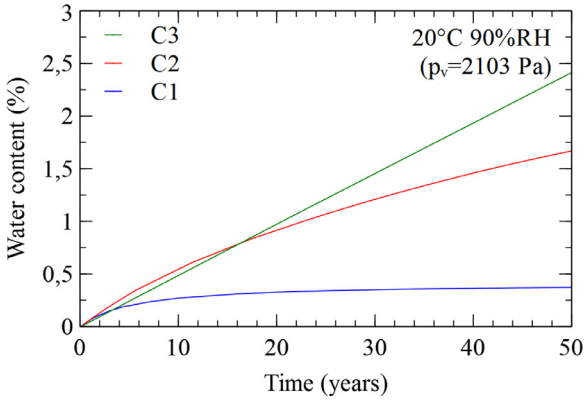

Fig. 9. Water content evolution of VIPs aged over 50 years, at 20 °C and 90% RH, with core materials C1, C2 and C3.

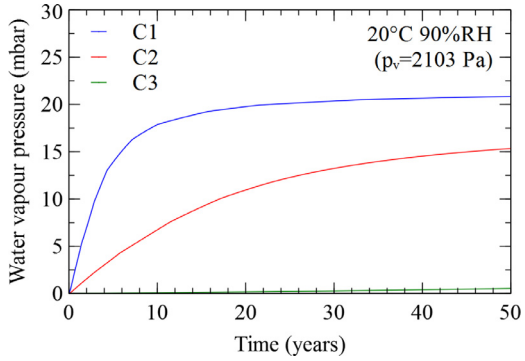

Fig. 10. Water vapour pressure evolution of VIPs aged over 50 years, at 20 °C and 90% RH, with core materials C1, C2 and C3.

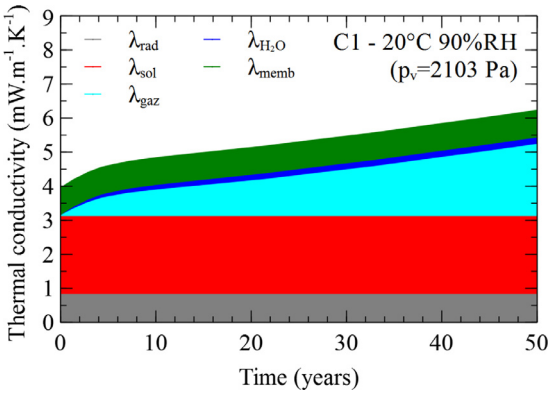

Fig. 11. Evolution of each thermal conductivity contribution of VIP aged over 50 years, at 20 °C and 90% RH, with core material C1.

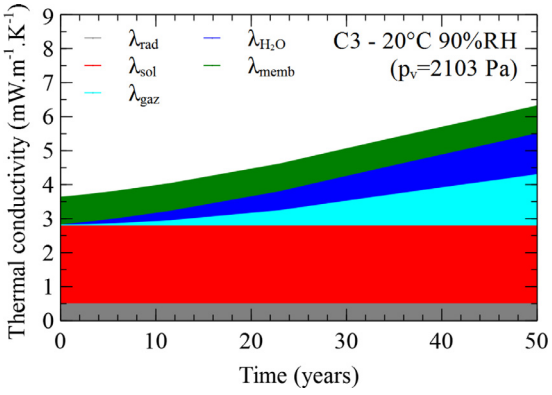

Fig. 12. Evolution of each thermal conductivity contribution of VIP aged over 50 years, at 20 °C and 90% RH, with core material C3.

ing flow of water vapour which results in a lower thermal conductivity increase.

At 40 °C (cf. Fig. 7) the differences between panels appear much more clearly and the increases of thermal conductivities are much more significant (increase between 6 and 13 mW m^{-1} K^{-1}). The thermal conductivity of the panel with more hydrophilic core material (C3) is lower than the others at the beginning of the ageing process, but rapidly, it exceeds all other conductivities (around 10 years) and always finishes with the higher value. After 50 years, thermal conductivity difference between panels with core material C1 and C3 depend on humidity condition. In contrast, difference between panels with core material C2 and C3 remains the same whatever the humidity condition.

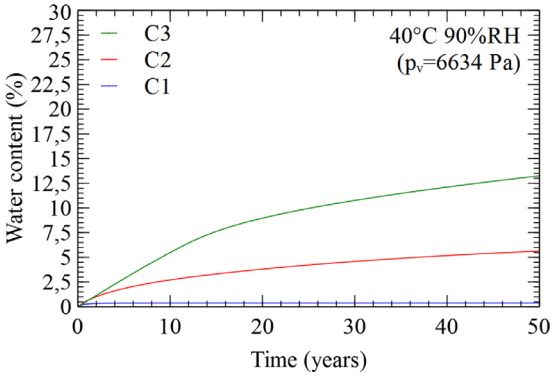

Fig. 13. Water content evolution of VIPs aged over 50 years, at 40 °C and 90% RH, with core materials C1, C2 and C3.

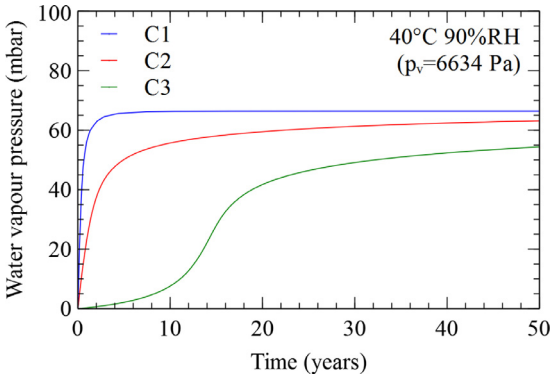

Fig. 14. Water vapour pressure evolution of VIPs aged over 50 years, at 40 °C and 90% RH, with core materials C1, C2 and C3.

As regards the hygric behaviour, core material C1 saturates even faster than core material C2 (cf. Fig. 13). After the first 10 years, the thermal conductivity evolutions seem to be identical for panel with core material C1 and C2 (cf. Fig. 7). An increasing difference actually arise with vapour partial pressure because core material C2 is not fully saturated.

The behaviour may also be explained by the observation of the water vapour partial pressure evolution (cf. Fig. 14). In panels with core material C1 and C2, the water vapour partial pressure increases very rapidly. In panel with core material C3, it remains very low during the first twenty years and then increases rapidly. In panel with core material C1, the water vapour partial pressure is in equilibrium with the external pressure after 4 or 5 years, while other panels never become saturated.

Consequently, at 40 °C and because of their very great difference of hygric behaviour, the VIPs made with hydrophobic core material has higher thermal conductivity in short term (until 20 years), but in long term they have the lowest one.

At 70 °C (cf. Fig. 8), the behaviours previously described are still amplified, but the core material C1 and C2 saturates promptly and water vapour partial pressure becomes in equilibrium with the external pressure. The thermal conductivity is mainly driven by the dry air pressure increase and the conductivity curves show parallel evolutions. The difference between VIPs thermal conductivities is controlled by water partial pressure. The VIPs made with hydrophobic core material always has lower thermal conductivity whatever the time after a few months.

To conclude, all simulations realised in constant conditions show the influence of the core material characteristics and of the external conditions severity on the long term thermal conductivity evolution. For low external water vapour partial pressure (<2200 Pa), hydrophilic core material is always favourable.

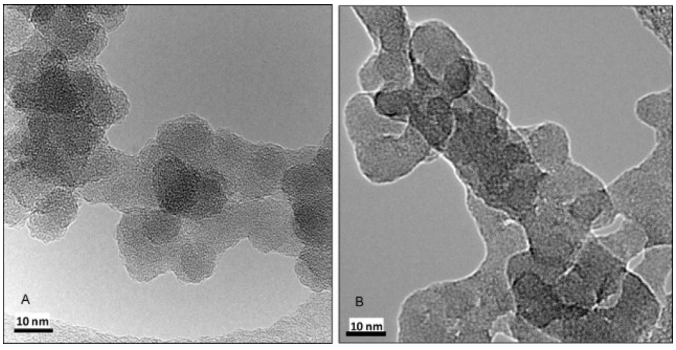

Fig. 15. Fumed silica (HDK T30® from Wacker) microstructure observed with TEM before (A), and after 205 days ageing at 60 °C and 80% RH (B) [3].

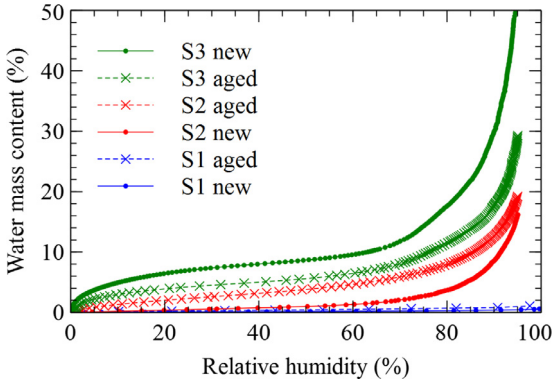

Fig. 16. Experimental water vapour sorption isotherms at 25 °C of new silica S1, S2 and S3, and aged after 24h at 70 °C and 90% RH then dried during 2h at 140 °C.

This is particularly true when the more hydrophilic core material has a lower initial thermal conductivity. For intermediate humidities (p_v between 2200 and 10,000 Pa), hydrophilic core materials can be preferred in short term (first 10 years) but they become unfavourable at long term. For high humidity condition ($p_v > 10$, 000 Pa), hydrophobic core materials are obviously more favourable.

6. Consideration of the silica ageing

6.1. Silica ageing

Until now, all simulations have been carried out on panels with fixed adsorption properties. For each core material one sorption isotherm was considered. It is now commonly admitted, thanks to many converging experimental statements [3–5], that the pore structure of all silica-based core materials change during the ageing process which results in an evolution of each material sorption isotherm.

Morel [3] have shown that during an ageing period, the specific surface area changes and is associated to a dissolution and re-precipitation mechanism of the silica primary particles (cf. Fig. 15). Even if the mechanisms responsible for these degradations remains not fully understood, an experimental evolution can be introduced in our model. The silica water vapour sorption isotherm evolution is considered.

For the three silica studied in this paper, water vapour sorption isotherms have been measured after 24 h ageing at 70 °C and 90% RH then dried during 2 h at 140 °C. The Fig. 16 shows the difference between sorption isotherms measured on silica at initial state (new) and after ageing (aged). It can be observed that silica S1 and S2 become more hydrophilic, whereas silica S3 becomes more hydrophobic.

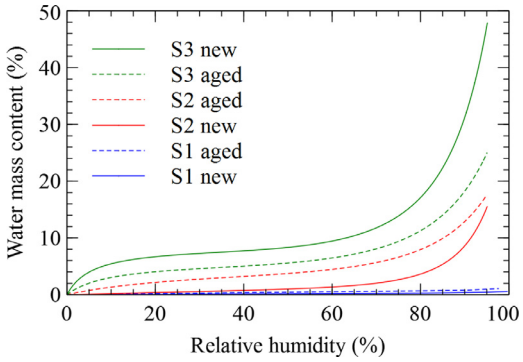

Fig. 17. Fitting water vapour sorption isotherms at 25 °C of new silica S1, S2 and S3, and aged after 24h ageing at 70 °C and 90% RH then dried during 2h at 140 °C.

Table 5
Fitting parameters for the water vapour sorption isotherms of studied silica in new condition and aged after 24h at 70 °C and 90% RH then dried during 2h at 140 °C.

Silica	k_1	k_2	k_3	k_4
S1 new	0.00777	1.83109	0.70576	5.43698
S1 aged	0.00711	0.43895	0.76642	2.43047
S2 new	0.11178	5.67065	2.90451	4.94117
S2 aged	0.05504	0.31095	1.79662	4.25848
S3 new	0.08714	0.06000	2.26808	4.99399
S3 aged	0.05957	0.09716	1.88530	4.11603

6.2. Silica ageing implementation

Sorption isotherms are implemented in the numerical model with the expression proposed in the Annex 39 (Eq. (37)) [25]. Sorption isotherms for new silica and silica at various stages of ageing have been fitted. Fig. 17 represents the sorption isotherms at 25 °C for silica S1, S2 and S3, at initial state (continuous curves) and fully aged after 24h at 70 °C and 90% RH then dried during 2h at 140 °C (dotted curves). Fitting parameters are recapped in Table 5.

To take into account the silica ageing, sorption isotherm moves from the new to the aged situation by changing the fitting parameter values. At time t, each parameter k_i is calculated as shown below:

$$k_i(t) = k_{i_{new}} - \left(\frac{min(t, t_{aged})}{t_{aged}}\right)^{\alpha} (k_{i_{new}} - k_{i_{aged}}) \quad (38)$$

t is the time, t_{aged} is the time for which the silica is considered as fully aged, and α is a parameter which allows to adapt the rate of ageing. α is a positive real coefficient. When α is equal to zero, sorption isotherm is considered as aged over all the simulation time. If α is different to zero, sorption isotherm moves from the new to the aged one. The higher α is, the later ageing is. A α value around 0.5 corresponds to a regular evolution of the sorption isotherm over all the ageing period. When α is very high, sorption isotherm is considered as always new but become rapidly aged just before t_{aged}. In both cases, silica is considered as fully aged when $t > t_{aged}$ and sorption isotherm no longer moves.

At all times, equilibrium is established between water vapour adsorbed by silica and water vapour in gaseous phase. At a given moment, if sorption isotherm changes, sorption equilibrium is disturbed. When sorption isotherm was fixed all over the time, adsorbed water was only a function of the relative humidity which depends on time (Eqs. (37) and (39)).

$$\tau_w(\phi) = f(\phi(t)) \quad (39)$$

But now, because sorption isotherm moves over the time, adsorbed water is a function of the relative humidity and of the fitting pa-

rameters which all depend on time (Eq. (40)).

$$\tau_w(t) = f(\phi(t), k_1(t), k_2(t), k_3(t), k_4(t)) \quad (40)$$

At each time step, the mass conservation of water into the panel has to be respected (Eqs. (41) and (42)).

$$dm_w = dm_{wv} + dm_{ads} \quad (41)$$

$$dm_w = \frac{M_{H_2O} \cdot \varepsilon V_{VIP}}{RT} dp_v + m_{sil} d\tau_w \quad (42)$$

Water mass content variation has to be calculated depending on relative humidity and fitting parameters variations. This requires to implement the total differential of sorption isotherm expression (Eq. (43)) which depends on its partial differentials with respect to the relative humidity and all of the fitting parameters.

$$\begin{aligned} d\tau_w = {} & \frac{k_1 e^{k_3\phi^{k_4}} (k_2 + k_2 k_3 k_4 \phi^{k_4} + k_3 k_4 \phi^{k_4+1})}{(k_2+\phi)^2} d\phi \\ & + \frac{\phi}{k_2+\phi} e^{k_3\phi^{k_4}} dk_1 - \frac{k_1\phi}{(k_2+\phi)^2} e^{k_3\phi^{d}} dk_2 \\ & + \frac{k_1\phi^{k_4+1}}{k_2+\phi} e^{k_3\phi^{k_4}} dk_3 + \frac{k_1 k_3 \phi^{k_4+1} ln(\phi)}{k_2+\phi} e^{k_3\phi^{k_4}} dk_4 \end{aligned} \quad (43)$$

7. Comparison between models taking in consideration or not silica ageing

The same simulations as in the previous paragraph are carried out, but with panels taking in consideration the silica ageing and panels with silica always considered as fully aged. For panels taking in consideration the silica ageing, silica are considered as fully aged at 25 years and it is supposed that the α parameter can be fixed to 0.07 for all conditions. This value has been determined according to experimental sorption isotherms evolution which are described in the Section 6.1.

The thermal conductivities evolution of VIPs aged over 50 years are presented on Figs. 18–20. For each condition, three curves are represented by core material (core materials C1, C2 and C3). The continuous curves correspond to panels always with the sorption isotherm of new silica (results already presented in Section 5). The dashed curves correspond to panels with the sorption isotherm of silica which are ageing over the time. The dotted curves correspond to panels always with the sorption isotherm of fully aged silica.

In rather dry conditions (at 20 °C and whatever the relative humidity), it can be observed that panels with core material C3 have the same thermal behaviour, whatever or not the silica ageing is taken into account. core material C3 is very hydrophilic but becomes more and more hydrophobic during the ageing process. When silica is ageing, an amount of adsorbed water becomes into the gaseous phase. Water in gaseous phase creates a lower thermal conductivity increase than when it is in adsorbed phase. The decrease of the thermal conductivity due to the adsorbed water balances with the increase of the gaseous thermal conductivity. In addition, the increase of water vapour partial pressure into the panel is significant compared to the external water vapour partial pressure. The water vapour partial pressure difference decreases and tends to diminish the water vapour flow which enter into the panel under this special condition with both side of the VIP at equal temperature. For panels with core material C2 and C1, the thermal conductivity difference is very low whatever or not the silica ageing is taken into account. The models taking into account the silica ageing over the time are very similar to the models always with fully aged silica.

In rather wet conditions (at 40 °C or 70 °C and whatever the relative humidity), it can be observed that the higher the external water vapour partial pressure is, the higher the difference is. The thermal conductivity difference is not significant for panels with core material C1. This was expected because core material C1 sorption isotherm doesn't changes very much when it is aged. For panels with core material C2 and C3, the difference is much more significant. When the silica ageing is taken into account, panel with core material C3 becomes favourable and panel with core material C2 becomes unfavourable. Again, models taking into account the silica ageing over the time are very similar to the models always with fully aged silica. In addition, it can be observed that when silica ageing is not taken into account the thermal conductivity difference between panels with core material C2 and C3 increases. In contrast, the difference decreases when the silica ageing is taken into account. In all cases, panels with core material C1 become more favourable in long term because core material C1 is the more hydrophobic one. Consequently, under this special condition with both side of the VIP at equal temperature, the water vapour partial pressure is rapidly in balance with the external one and only allows dry air to pass through the envelope which has the lower dry air permeance than water vapour.

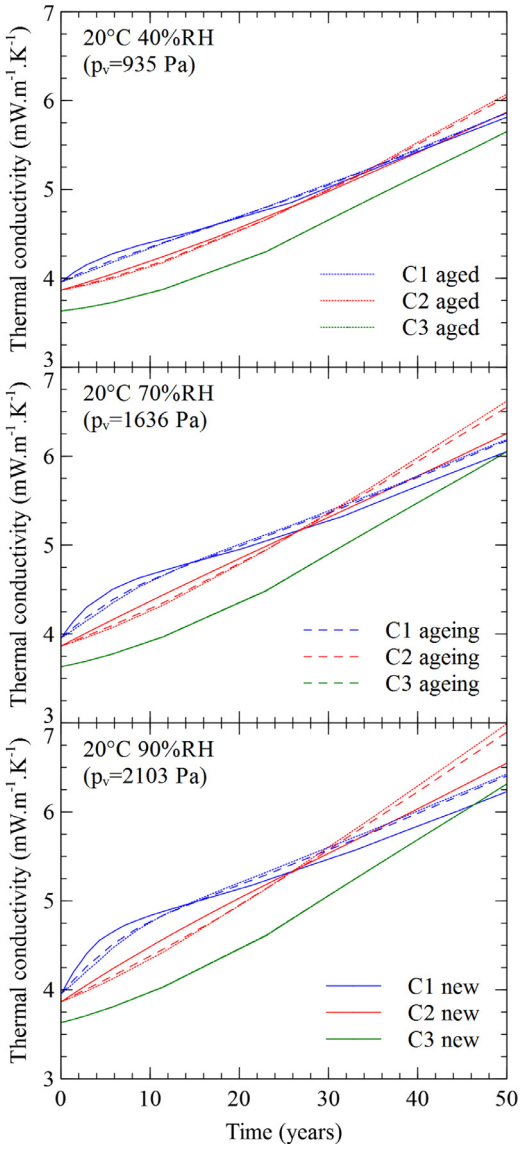

Fig. 18. Thermal conductivities evolution of VIPs aged over 50 years at 20 °C for 40, 70 and 90% RH, with core materials C1, C2 and C3 always new (continuous curves), ageing over the time (dashed curves) and always aged (dotted curves).

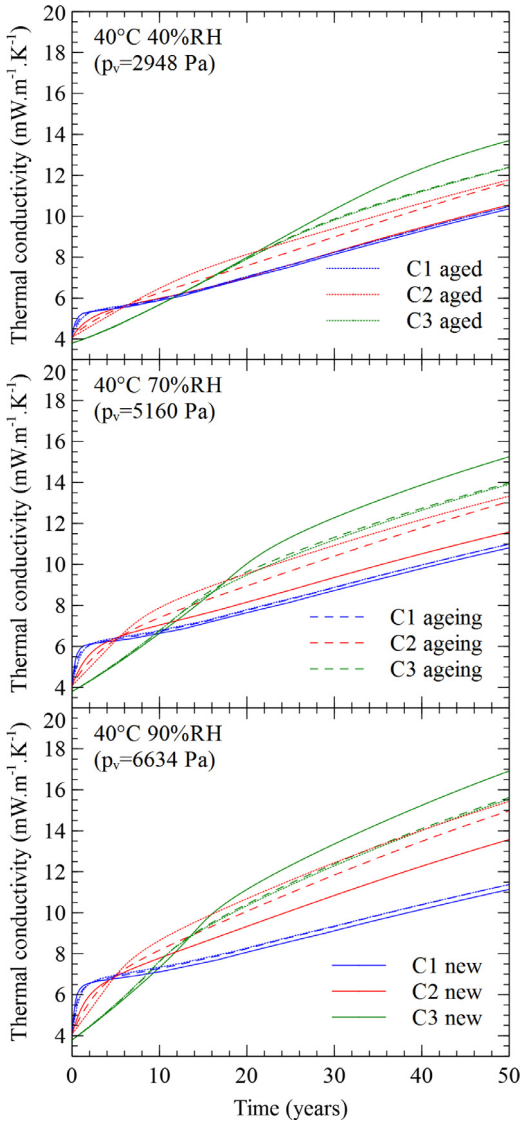

Fig. 19. Thermal conductivities evolution of VIPs aged over 50 years at 40 °C for 40, 70 and 90% RH, with core materials C1, C2 and C3 always new (continuous curves), ageing over the time (dashed curves) and always aged (dotted curves).

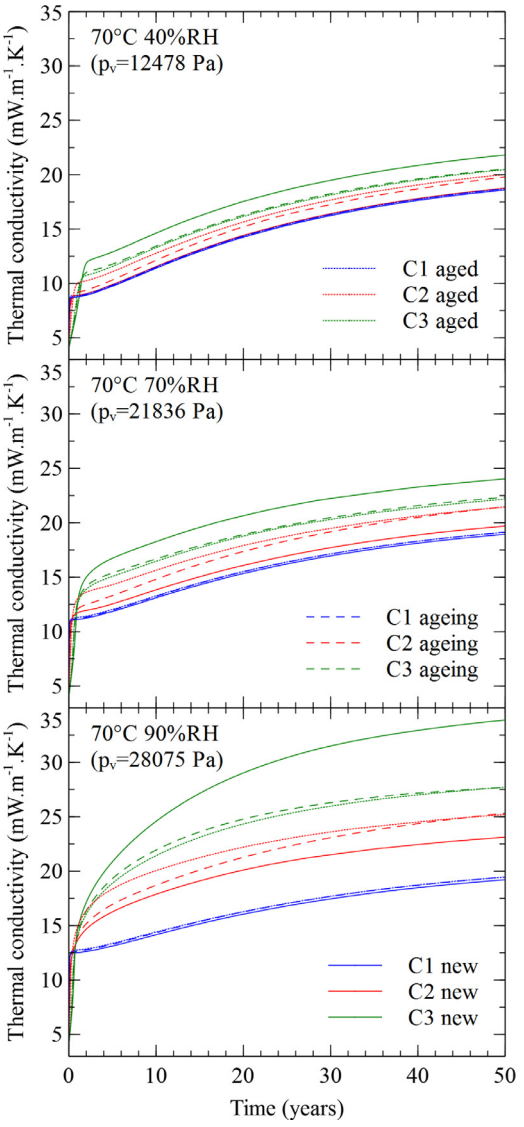

Fig. 20. Thermal conductivities evolution of VIPs aged over 50 years at 70 °C for 40, 70 and 90% RH, with core materials C1, C2 and C3 always new (continuous curves), ageing over the time (dashed curves) and always aged (dotted curves).

8. Model validation and discussion about traditional ageing prediction

8.1. Case study presentation

The results presented in this part are based on a very helpful case study managed by EMPA in Switzerland. For VIPs evaluation, tests are generally carried out during short term period (some weeks, or some months) in very severe conditions for accelerating the ageing phenomena. The case study of EMPA is very different as the tests have been carried out over 10 years in relatively mild conditions.

Four panels had been tested in two different conditions: a fixed temperature of 23 °C and two relative humidities: 33% and 80%. These tests are summarized in Table 6.

Panels have been manufactured by va-Q-tec®. The barrier complex is a three-metallized film from Hanita® and core material is made with fumed silica S2. The silica density is 195 kg m^{-3}, its porosity is fixed at 93.5% and the mean pore size is around 260 nm. The determination of some panels characteristics at initial conditions and after ageing (thermal conductivity, internal total pressure and water content) have been carried out at EMPA [8,35]. The results are presented in Table 7.

Table 6
Characteristics of VIPs stored at EMPA and solicitations.

N°	Size (cm^3)	Conditions	Start	End
12 13	50 × 50 × 2	23 °C 33% RH	19/05/2003	31/03/2014
6 7	50 × 50 × 2	23 °C 80% RH	27/07/2003	31/03/2014

After ageing, the panels have been analysed by EDF's laboratories [36]. Water vapour sorption isotherms have been measured on core materials and apparent permeances have been calculated from pressure increases.

Fig. 21 shows water vapour sorption isotherms for new silica S2 (blue curve), fully aged silica S2 (green curve), and silica S2 after 10 years of storage at EMPA at 23 °C/33% RH and 23 °C/80% RH (black curves). It has been concluded that the core materials were not fully aged after 10 years of ageing.

Table 7
Thermal conductivity, internal total pressure and water content measurements realised by EMPA on VIPs stored at EMPA at 23 °C/33% RH and 23 °C/80% RH.

EMPA	23 °C 33% RH	23 °C 80% RH
$\lambda_{VIP,\ init}$ (mW m^{-1}K^{-1})	3.9	3.9
$\lambda_{VIP,\ after\ 10\,y}$ (mW m^{-1}K^{-1})	4.5	6.1
$p_{t,\ init}$ (mbar)	1	1
$p_{t,\ after\ 10\,y}$ (mbar)	6	18.5
$\tau_{w,\ init}$ (%)	0.1	0.1
$\tau_{w,\ after\ 10\,y}$ (%)	0.6	3.1

Table 8
Apparent permeances measurements realised by EDF after 10 years of storage at EMPA at 23 °C/33% RH and 23 °C/80% RH.

EDF	23 °C 33% RH	23 °C 80% RH
Π_{wv} (kg m^{-2} s^{-1}Pa^{-1})	3.2×10^{-14}	7.4×10^{-14}
Π_{air} (kg m−2s^{-1}Pa^{-1})	1.5×10^{-18}	5.2×10^{-18}

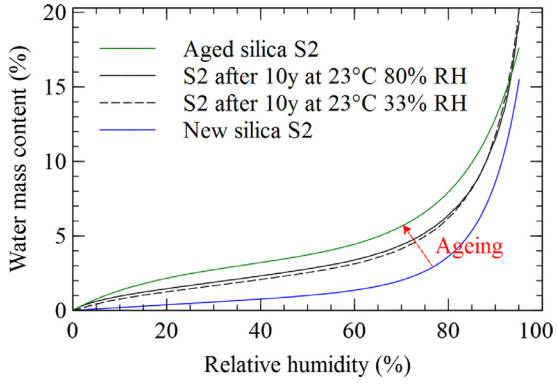

Fig. 21. Water vapour sorption isotherms at 25 °C of new silica S2, aged silica S2 and silica S2 after 10 years of storage at EMPA at 23 °C/33% RH and 23 °C/80% RH. (For interpretation of the references to color in the text, the reader is referred to the web version of this article.)

8.2. Model validation

The measurements made it possible to configure the numerical model and make simulations of panels over 25 years in actual testing conditions. Two hypothesis have been adopted: permeances values are those calculated at the end of tests, and silica are considered as fully aged at 25 years.

For both experimental conditions, three sets of simulations have been carried out with three hypothesis concerning the core material ageing. These hypothesis are the same than those used in the previous paragraph: one panel has always a new silica (blue curves), one panel has a silica which is ageing over the time (red curves) and one panel has always a fully aged silica (green curves). So, all simulated panels are the same but only differ in the adopted hypothesis concerning the sorption isotherm of their core material.

For panel with sorption isotherm which change over the time, the parameter α which represents the rate of ageing is calculated such that the calculated sorption isotherm after 10 years of ageing corresponds to the experimental one. α is estimated at 0.10 and 0.07 for panels stored at 33 and 80% RH respectively. These values are lower than 0.5 and mean that silica sorption isotherm changes mostly at the beginning than at the end of the ageing process. The parameter α for panels stored at 80% RH is lower than for panels stored at 33% RH. This means that the ageing process is accelerated by humidity.

Simulation results are presented from Figs. 22 to 24 for panels stored at 33% RH, and from Figs. 25 to 27 for panels stored at 80% RH. Measurements realised at EMPA are represented on graphs

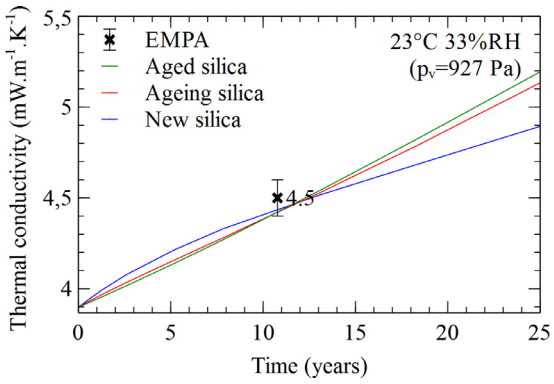

Fig. 22. Thermal conductivity evolution of VIPs stored at EMPA over 25 years at 23 °C and 33% RH. (For interpretation of the references to color in the text, the reader is referred to the web version of this article.)

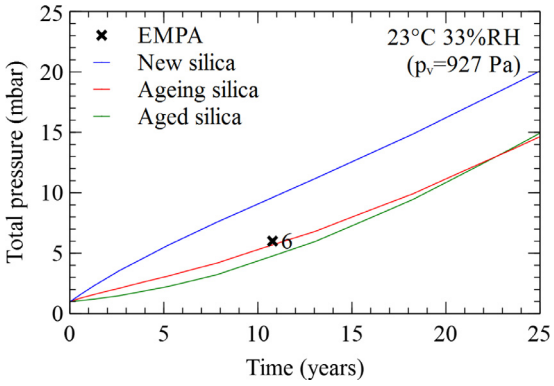

Fig. 23. Total pressure evolution of VIPs stored at EMPA over 25 years at 23 °C and 33% RH. (For interpretation of the references to color in the text, the reader is referred to the web version of this article.)

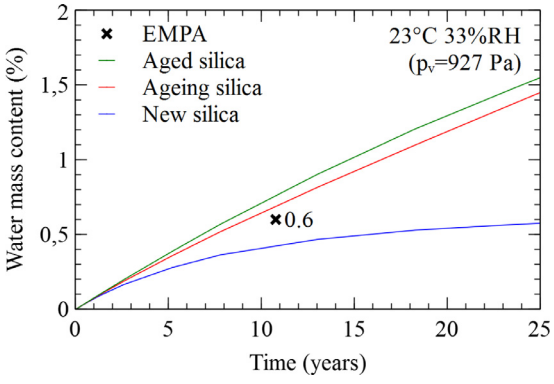

Fig. 24. Water content evolution of VIPs stored at EMPA over 25 years at 23 °C and 33% RH. (For interpretation of the references to color in the text, the reader is referred to the web version of this article.)

by a cross. In both conditions, results show a good agreement between measured characteristics (thermal conductivity, internal total pressure and water mass content) at 10 years and the simulated results when silica ageing process is considered (red curves).

There is a very little difference between panels with ageing silica (red curves) and with aged silica (green curves), but the model taking into account the ageing process is always closer to the model with fully aged silica than the model with new silica.

At 23 °C and 33% RH (Figs. 22–24), after 10 years it can be observed that the thermal conductivities difference increases, but values stay very close after 25 years ($\Delta\lambda_{VIP} < 0.3$ mW m^{-1} K^{-1}). The panels with new and aged silica are in agreement with the mea-

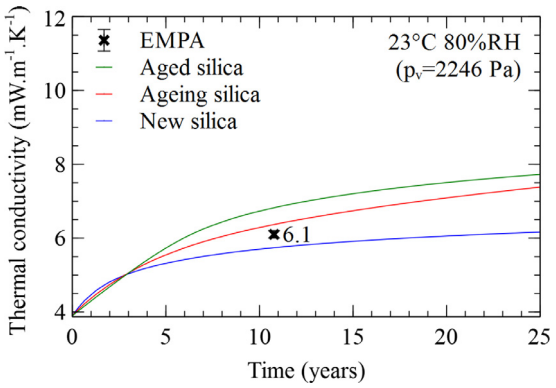

Fig. 25. Thermal conductivity evolution of VIPs stored at EMPA over 25 years at 23 °C and 80% RH. (For interpretation of the references to color in the text, the reader is referred to the web version of this article.)

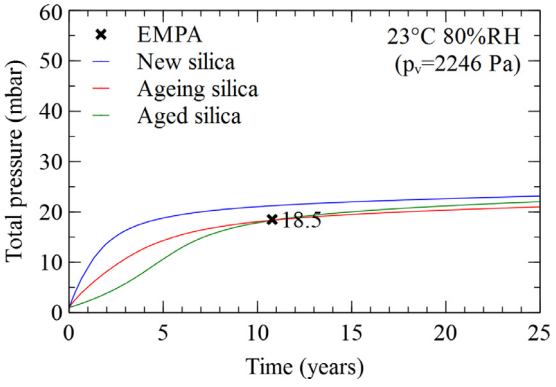

Fig. 26. Total pressure evolution of VIPs stored at EMPA over 25 years at 23 °C and 80% RH. (For interpretation of the references to color in the text, the reader is referred to the web version of this article.)

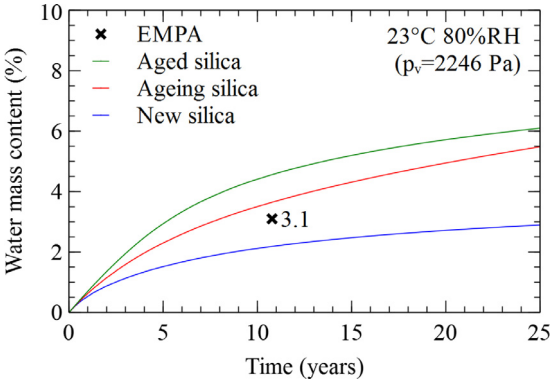

Fig. 27. Water content evolution of VIPs stored at EMPA over 25 years at 23 °C and 80% RH. (For interpretation of the references to color in the text, the reader is referred to the web version of this article.)

sured thermal conductivity, but not with the total pressure and the water content measurements.

At 23 °C and 80% RH (Figs. 25–27), panels with new and aged silica can't not represent the real panels' behaviour with regard to the thermal conductivity, the total pressure and the mass content.

All results show that the dynamic model developed allow to fairly mimic the measurements despite the uncertainty in some inputs parameters (permeances, porosity, mean pore size, rate of ageing of silica, etc.) The silica ageing process is mandatory to correctly simulate the panel's behaviour.

Table 9
Pressure and water content yearly rates measured by EMPA on VIPs stored over 10 years at 23 °C/33% RH and 23 °C/80% RH

Conditions	23 °C 33% RH	23 °C 80% RH
Δp_t (mbar year^{-1})	0.56	1.8
$\Delta \tau_w$ (% year^{-1})	0.05	0.3

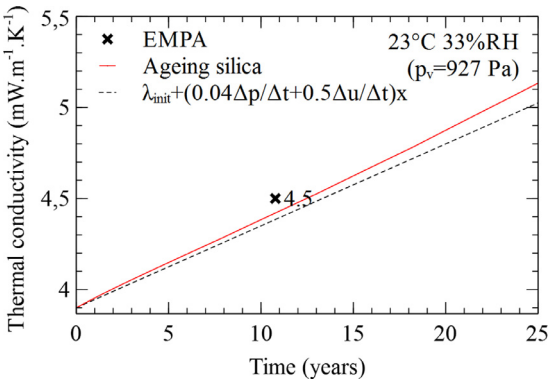

Fig. 28. Thermal conductivity evolution of VIPs stored at EMPA over 25 years at 23 °C and 33% RH, comparison with linear ageing prediction.

8.3. Comparison with traditional ageing prediction

8.3.1. Linear model description

To predict the long term thermal behaviour of VIPs, a linear model (Eq. (45)) is commonly used by many authors [8,10,11,17,33,34]. Thermal conductivity is calculated from the pressure and the water content increase which are measured by short term testing. The influence of pressure increase on the thermal conductivity is represented by the experimental G parameter, and that of the water content increase by the *B* parameter.

$$\Delta\lambda_{VIP} = \frac{\partial\lambda_{VIP}(p_t)}{\partial p_t}\Delta p_t + \frac{\partial\lambda_{VIP}(\tau_w)}{\partial \tau_w}\Delta\tau_w \tag{44}$$

$$= G\cdot\Delta p_t + B\cdot\Delta\tau_w \tag{45}$$

It seems interesting to compare the dynamic model prediction presented in this paper to the linear ageing prediction method. The case study of the 10 years storage of VIPs at EMPA previously presented is used.

Regarding the 10 years ageing tests carried out at EMPA, the annual gas pressure and water content increases can be evaluated for both testing conditions (cf. Table 9).

Parameters G and *B* have been determined with short term tests, and estimated as well [17,37]:

$G = 0.04$ mW m^{-1} K^{-1} mbar^{-1}

$B = 0.5$ mW m^{-1} K^{-1}%$^{-1}$

Linear model estimates the thermal conductivity increase at 0.045 and 0.222 mW m^{-1} K^{-1} per year for panels stored at 23 °C/33% RH and 23 °C/80% RH respectively [36].

8.3.2. Comparison over 25 years

The linear approximation of the thermal conductivity value can then be expanded over 25 years and compared to our simulation results (cf. Figs. 28–33). As shown in Section 8.2, the panel's behaviour can be correctly simulated only with the model taking into account the silica ageing. Only simulation results of this model are represented on graphs.

At 23 °C and 33% RH (cf. Figs. 28–30), dynamic model taking into account ageing of silica and linear model are very close. We

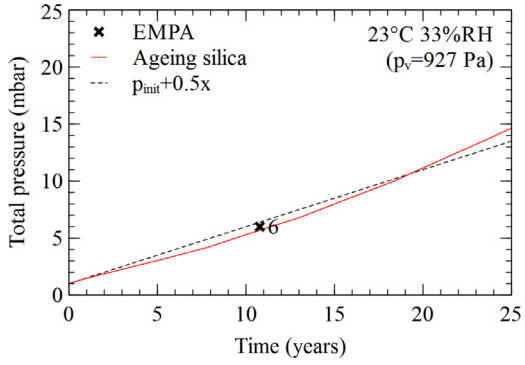

Fig. 29. Total pressure evolution of VIPs stored at EMPA over 25 years at 23 °C and 33% RH, comparison with linear ageing prediction.

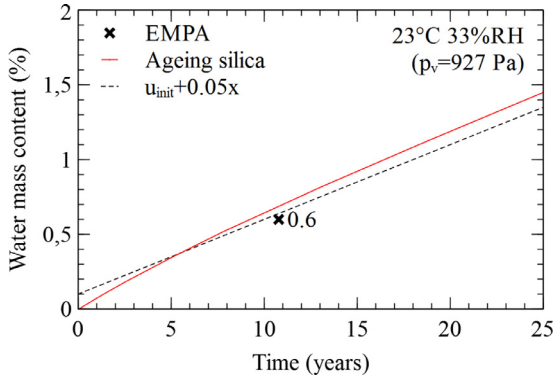

Fig. 30. Water content evolution of VIPs stored at EMPA over 25 years at 23 °C and 33% RH, comparison with linear ageing prediction.

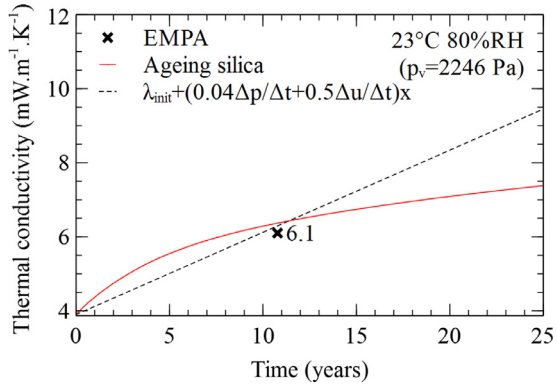

Fig. 31. Thermal conductivity evolution of VIPs stored at EMPA over 25 years at 23 °C and 80% RH, comparison with linear ageing prediction.

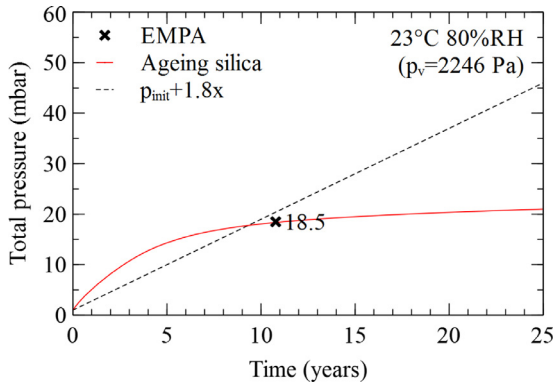

Fig. 32. Total pressure evolution of VIPs stored at EMPA over 25 years at 23 °C and 80% RH, comparison with linear ageing prediction.

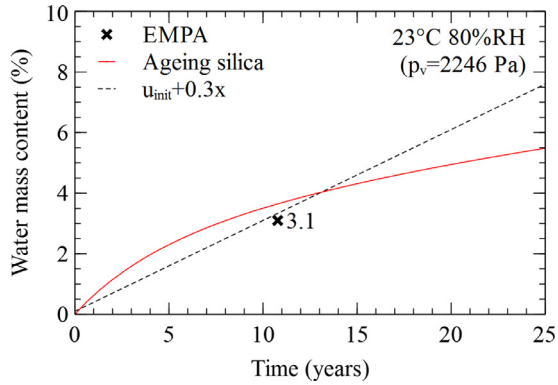

Fig. 33. Water content evolution of VIPs stored at EMPA over 25 years at 23 °C and 80% RH, comparison with linear ageing prediction.

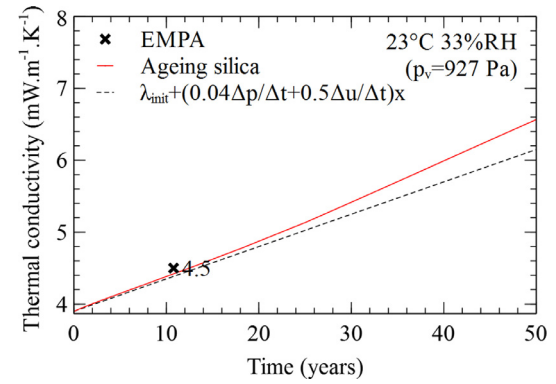

Fig. 34. Thermal conductivity evolution of VIPs stored at EMPA over 50 years at 23 °C and 33% RH, comparison with linear ageing prediction.

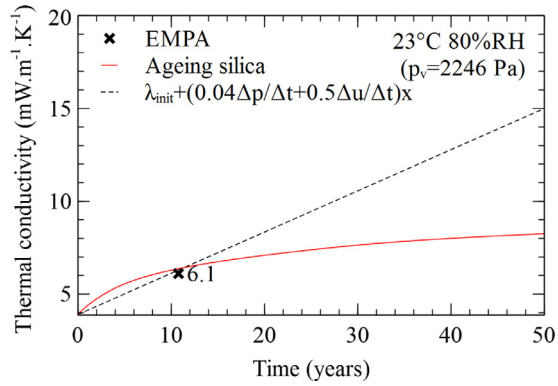

Fig. 35. Water content evolution of VIPs stored at EMPA over 25 years at 23 °C and 80% RH, comparison with linear ageing prediction.

can see that linear model underestimate the pressure increase and overestimate the water content increase. The two effects balance each other and the predicted thermal conductivity can be correct (after 25 years, $\Delta\lambda_{VIP_{linear/simu}} \approx 0.2$ mW m^{-1} K^{-1}).

At 23 °C and 80% RH (cf. Figs. 31–33), linear model tends to overestimate the pressure and the water content increase. Linear model cannot predict correctly the thermal conductivity evolution and predicts too high values (after 25 years, $\Delta\lambda_{VIP_{linear/simu}} \approx$ 2 mW m^{-1} K^{-1}).

8.3.3. Comparison over 50 years

Same simulations are realised over 50 years in order to compare the models in long term (cf. Figs. 34 and 35).

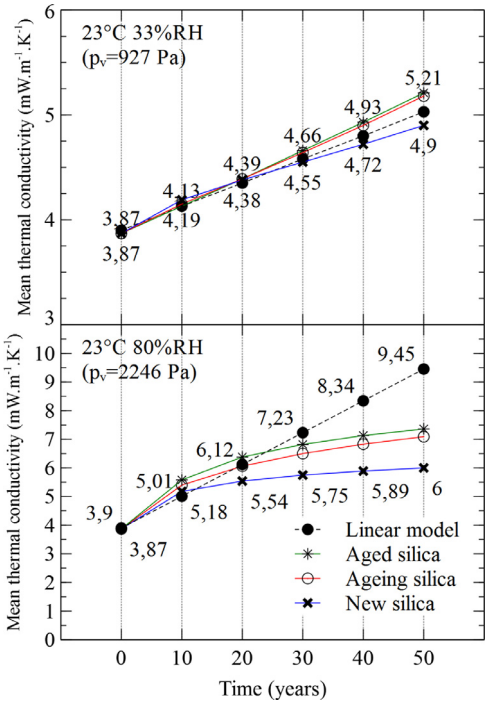

Fig. 36. Mean thermal conductivity of VIPs stored at EMPA over 50 years, at 23 °C/33% RH and 23 °C/80% RH, calculated at 0, 10, 20, 30, 40 and 50 years, comparison with linear ageing prediction.

Similar trend are observed over 50 years with more pronounced differences. In dry conditions, linear model always underestimates the thermal conductivity (after 50 years, $\Delta\lambda_{VIP_{linear/simu}} \approx 0.4$ mW m^{-1} K^{-1}). In wet conditions, linear model underestimates the thermal conductivity in short term, but much more overestimate it in long term (after 50 years, $\Delta\lambda_{VIP_{linear/simu}} \approx 7$ mW m^{-1} K^{-1}).

The mean thermal conductivity of panels are calculated for each condition and at different times of ageing process: 0, 10, 20, 30, 40 and 50 years (cf. Fig. 36). Linear model and the dynamic model with the three hypothesis about its core material ageing are represented.

It can be observed that in dry conditions (at 23 °C and 33% RH), linear model gives mean thermal conductivity values close to those of dynamic model even if it cannot predict the real panel behaviour. The difference between all models is less than 0.3 mW m^{-1} K^{-1} and is not significant.

In wet conditions (at 23 °C and 80% RH), linear model gives mean thermal conductivities close to those of dynamic model only over the first 20 years. After 20 years, linear model overestimated the mean thermal conductivity and is unfavourable. The difference between models is not negligible. Over 50 years, linear model predicts a mean thermal conductivity at least 2 mW m^{-1} K^{-1} higher than the most pessimistic dynamic model.

8.4. Comparison with linear model in very wet conditions

As shown in Section 5, the influence of the external water vapour partial pressure on the long term thermal conductivity evolution is very important. Simulations of VIPs stored at EMPA are not exposed to very wet conditions. Simulations over 50 years at 40 °C and 80% RH with the same panels have been carried out in wetter conditions ($p_v = 5897$ Pa).

From simulation results with the dynamic model taking into account the silica ageing, pressure and water content increases are calculated (after 10 years) and used as inputs for linear model. Mean thermal conductivities are presented on Fig. 37.

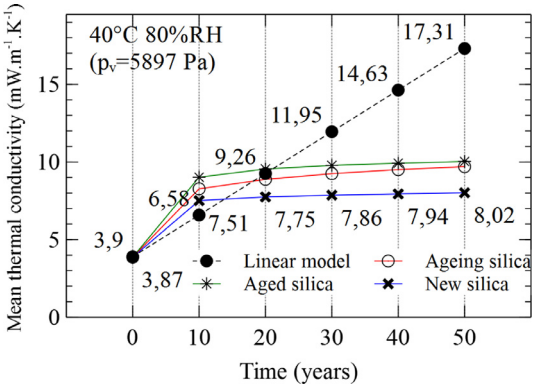

Fig. 37. Mean thermal conductivity of VIPs over 50 years, at 40 °C/80% RH, calculated at 0, 10, 20, 30, 40 and 50 years, comparison with linear ageing prediction.

It can be observed that the linear model underestimates the mean thermal conductivity over the first 20 years, and overestimates it after 20 years. Differences between linear and dynamic models are higher than in previous conditions (after 50 years, $\Delta\lambda_{VIP_{linear/simu}} \approx 7$ mW m^{-1} K^{-1}).

9. Conclusions and outlook

The dynamic model presented in this paper gives simulation results which seem in accordance with experimental results and offers a good accuracy. Thanks to this model, the panels dynamic behaviour and ageing can be anticipated for various panels configurations and ageing conditions. Simulations have shown that the silica ageing has a significant impact on the thermal conductivity evolution. If silica is supposed to keep its initial characteristics, simulation results are obviously very optimistic regarding the long term conductivity. In contrast, considering a fully aged silica during all the ageing process gives reasonably correct results. Results will be a slightly unfavourable, but not very different from measured conductivities.

The ageing mechanism is more complex than that of condidered in this model. For the silica S2, its sorption isotherm becomes more hydrophobic at the end of its ageing. More research work is required to better understand and take into account this mechanism.

In rather dry conditions, the linear model can be a reasonable estimation of the mean thermal conductivity. But the pressure and water content evolutions are significantly far from their measured values. In wetter conditions, the linear model underestimates the short term mean thermal conductivity and overestimates the long term one. Consequently, short term measurements don't allow to predict and understand the long term behaviour with the linear model, but they allow to check dynamic models.

All results show that the crucial factor is water vapour partial pressure and not relative humidity. Low temperature and wet conditions are less unfavourable than high temperature and dry conditions. The silica ageing being faster for panels in wet conditions than those in dry conditions, this is in accordance with the hypothesis that the silica ageing is driven by the water vapour which enters into the VIP. The silica ageing mechanisms could be directly related to the water mass inside the panel.

Thanks to the dynamic model, the most crucial VIPs' characteristics for the long term thermal conductivity have been determined regarding the solicitations. With a view to a normalisation for building insulation applications, it would be much more judicious to set performance levels on these characteristics regarding

the applications, rather than setting performance levels on initial or mean thermal conductivities. Indeed these thermal conductivities values are always measured in short term and are not representative of the long term behaviour.

Simulations carried out in constant conditions show the importance of external temperature and humidity conditions. That is why it is necessary to study the VIPs behaviour with real solicitations in service life. This is the aim of another paper which proposes a new method in order to determine temperatures and humidities at the panels' surface when they are installed in systems for various building insulation applications.

Acknowledgements

The authors gratefully acknowledge the collaborators of the project EMMA-PIV (no. ANR 12-VBDU-0004-01) that includes this research, and also the National Research Agency (ANR) for his financial support. This work is performed within the framework of the Centre of Excellence of Multifunctional Architectured Materials "CEMAM" no. AN-10-LABX-44-01.

References

[1] G. Garnier, Conception et Optimisation des Enveloppes Pour Super-Isolants Thermiques Sous Vide, Ph.D. thesis, Institut National Polytechnique de Grenoble, 2009.
[2] M. Bouquerel, T. Duforestel, D. Baillis, F. Kuznik, Mass transfer in the envelope of vacuum insulation panels, a modeling challenge for aging prediction, 10th International Vacuum Insulation Symposium – IVIS, Ottawa, Canada, 2011.
[3] B. Morel, Vieillissement Thermohydrique de Silices Nanométriques, Ph.D. thesis, Université François-Rabelais de Tours, 2008.
[4] B. Morel, L. Autissier, D. Autissier, D. Lemordant, B. Yrieix, D. Quenard, Pyrogenic silica ageing under humid atmosphere, Powder Technol. 190 (1–2) (2009) 225–229, doi:10.1016/j.powtec.2008.04.049.
[5] B. Yrieix, B. Morel, E. Pons, Vip service life assessment: interactions between barrier laminates and core material, and significance of silica core ageing, Energy Build. 85 (2014) 1–26, doi:10.1016/j.enbuild.2014.07.035.
[6] B. Morel, Modifications of a pyrogenic silica exposed to moist air, in: 8th International Vacuum Insulation Symposium – IVIS, Würzburg, Germany, 2007, pp. 1–18.
[7] M. Bouquerel, T. Duforestel, D. Baillis, G. Rusaouen, Heat transfer modeling in vacuum insulation panels containing nanoporous silicas – a review, Energy Build 54 (2012) 320–336, doi:10.1016/j.enbuild.2012.07.034.
[8] R. Caps, I. Wallaschek, I. Abu-Shawriyeh, H. Beyrichen, S. Brunner, Evaluation of thermal conductivity increase of vips, in: Annex 65 Meeting, Nanjing (China), 2015.
[9] H. Schwab, U. Heinemann, A. Beck, H.-P. Ebert, J. Fricke, Dependence of thermal conductivity on water content in vacuum insulation panels with fumed silica kernels, J. Therm. Envelope Build. Sci. 28 (4) (2005) 319–326, doi:10.1177/1097196305051792.
[10] U. Heinemann, Influence of water on the total heat transfer in 'evacuated' insulations, Int. J. Thermophys. 29 (2) (2008) 735–749, doi:10.1007/s10765-007-0361-1.
[11] H. Schwab, U. Heinemann, J. Wachtel, H.-P. Ebert, J. Fricke, Predictions for the increase in pressure and water content of vacuum insulation panels (vips) integrated into building constructions using model calculations, J. Therm. Envelope Build. Sci. 28 (4) (2005) 327–344, doi:10.1177/1097196305051793.
[12] H. Schwab, U. Heinemann, A. Beck, H.-P. Ebert, J. Fricke, Prediction of service life for vacuum insulation panels with fumed silica kernel and foil cover, J. Therm. Envelope Build. Sci. 28 (4) (2005) 357–374, doi:10.1177/1097196305051894.
[13] M.J. Tenpierik, H. Cauberg, Simplified analytical models for service life prediction of a vacuum insulation panel, 8th International Vacuum Insulation Symposium – IVIS, Würzburg, Germany, 2007.
[14] S. Brunner, H. Simmler, Service life prediction for vacuum insulation panels (vip), in: CISBAT 2003 Conference, EPFL, Lausanne, Switzerland, 2003.
[15] M. Tenpierik, W. van der Spoel, J. Cauberg, Analytical model for computing thermal bridge effects in high performance building panels, in: Carsten Rode (Ed.), 8th Symposium on Building Physics in the Nordic Countries, Technical University of Denmark, 2008, pp. 9–16.
[16] E. Wegger, B. Jelle, E. Sveipe, S. Grynning, R. Baetens, J.V. Thue, Effect of ageing on service life of vacuum insulation panels, Build. Enclosure Sci. Technol. (BEST 2 – 2010) (2010) 6–7.
[17] H. Simmler, S. Brunner, Vacuum insulation panels for building application: basic properties, aging mechanisms and service life, Energy Build. 37 (11 SPEC. ISS.) (2005) 1122–1131, doi:10.1016/j.enbuild.2005.06.015.
[18] D. Quénard, H. Sallée, Micro-nano porous materials for high performance thermal insulation micro-nano porous materials for high performance, in: 2nd International Symposium on Nanotechnology in Construction, Bilbao, Spain, 2005, pp. 0–10.
[19] J. Fricke, E. Hémmer, H.-J. Morper, P. Scheuerpflug, Thermal properties of silica aerogels, Revue de Physique Appliquée 24 (4) (1989) C487—-C497, doi:10.1051/jphyscol:1989414.
[20] T. Rettelbach, J. Säuberlich, S. Korder, J. Fricke, Thermal conductivity of silica aerogel powders at temperatures from 10 to 275 k, J. Non Cryst. Solids 186 (1995) 278–284, doi:10.1016/0022-3093(95)00051-8.
[21] U. Heinemann, R. Caps, J. Fricke, Radiation-conduction interaction : an investigation on silica aerogels, Int. J. Heat Mass Transf. 39 (10) (1996) 2115–2130, doi:10.1016/0017-9310(95)00313-4.
[22] R. Caps, J. Fricke, Thermal conductivity of opacified powder filler materials for vacuum insulations, Int. J. Thermophys. 21 (2) (2000) 445–452, doi:10.1023/A:1006691731253.
[23] K. Kamiuto, Combined conductive and radiative heat transfer through evacuated silica aerogel layers, Int. J. Solar Energy 9 (1) (1990) 23–33, doi:10.1080/01425919008941471.
[24] J. Blahovec, S. Yanniotis, Gab generalized equation for sorption phenomena, Food Bioproc. Tech. 1 (1) (2008) 82–90, doi:10.1007/s11947-007-0012-3.
[25] M. Erb, H. Simmler, S. Brunner, U. Heinemann, H. Schwab, K. Kumaran, P. Mukhopadhyaya, D. Quénard, H. Sallée, K. Noller, E. Kücükpinar-Niarchos, C. Stramm, M.T.H. Cauberg, Vacuum Insulation Panels – Study on VIP-components and Panels for Service Life - Prediction of VIP in Building Applications (Subtask A), Technical Report, September 2005, HiPTI – High Performance Thermal Insulation – IEA/ECBCS Annex 39, 2005.
[26] M.G. Kaganer, Thermal insulation in cryogenic engineering, Israel program for scientific translations, Jerusalem (1969) (1969).
[27] V. Stannett, Simple gases, in diffusion in polymers, Crank, J. and Park (1968) 41–73.
[28] H.B. Hopfenberg, V. Stannett, The Diffusion and Sorption of Gases and Vapours in Glassy Polymers, Springer Netherlands, Dordrecht, pp. 504–547.
[29] B. Flaconneche, J. Martin, M.H. Klopffer, Permeability, diffusion and solubility of gases in polyethylene, polyamide 11 and poly (vinylidene fluoride), Oil Gas Sci. Technol. 56 (3) (2001) 261–278, doi:10.2516/ogst:2001023.
[30] E. Shufer, MVTR As a Function of Temperature and Relative Humidity, TR, Hanita Coating, 2015.
[31] M. Erb, U. Heinemann, H. Schwab, H. Simmler, S. Brunner, K. Ghazi, R. Bundi, K. Kumaran, P. Mukhopadhyaya, D. Quénard, H. Sallée, K. Noller, E.K.-N. and-Cornelia Stramm, M. Tenpierik, H. Cauberg, A. Binz, G. Steinke, A. Moosmann, Vacuum Insulation – Panel Properties and Building Applications – Summary, Technical Report, December 2005, HiPTI – High Performance Thermal Insulation – IEA/ECBCS Annex 39, 2005.
[32] M. Bouquerel, T. Duforestel, D. Baillis, G. Rusaouen, Mass transfer modeling in gas barrier envelopes for vacuum insulation panels: a review, Energy Build. 55 (2012) 903–920, doi:10.1016/j.enbuild.2012.09.004.
[33] E. Pons, B. Yrieix, L. Heymans, F. Dubelley, E. Planes, Permeation of water vapor through high performance laminates for vips and physical characterization of sorption and diffusion phenomena, Energy Build. 85 (2015) 604–616, doi:10.1016/j.enbuild.2014.08.032.
[34] H. Schwab, U. Heinemann, A. Beck, H.-P. Ebert, J. Fricke, Permeation of different gases through foils used as envelopes for vacuum insulation panels, J. Therm. Envelope Build. Sci. 28 (4) (2005) 293–317, doi:10.1177/1097196305051791.
[35] R. Caps, I. Wallaschek, I. Abu-Shawriyeh, S. Brunner, Methods for evaluation of thermal conductivity increase of vips, 12th International Vacuum Insulation Symposium – IVIS, Nanjing (China), 2015.
[36] S. Brunner, B. Yrieix, E. Pons, Evaluation of vips after mild artificial aging during 10 years: focus on the core behavior, 12th International Vacuum Insulation Symposium – IVIS, Nanjing (China), 2015.
[37] H. Schwab, Vakuumisolationspaneele- Gas- und Feuchteeintrag sowie Feuchte- und Wärmetransport, Ph.D. thesis, Julius-Maximilians-Universität Würzburg, Würzburg, Germany, 2004.